ACS OMEGA

Open Access

http://pubs.acs.org/journal/acsodf

Article

Network Pharmacology-Based Strategy Integrated with Molecular Docking and In Vitro Experimental Validation to Explore the Underlying Mechanism of *Fangji Huangqi* Decoction in Treating Rheumatoid Arthritis

Weijin Zhang,[§] Hui Guo,[§] Leyuan Li, Mengmeng Zhang, Erping Xu, and Liping Dai*

Cite This: *ACS Omega* 2024, 9, 31878−31889

Read Online

ACCESS | Metrics & More | Article Recommendations

ABSTRACT: *Fangji Huangqi* decoction (FHD), as a classic traditional Chinese medicine formula, has been clinically proven effective against rheumatoid arthritis (RA), yet its therapeutic mechanism remains unclear. This study employed network pharmacology and molecular docking methods to explore the major active components, biological targets, and signaling pathways of FHD. Subsequently, lipopolysaccharide (LPS)-stimulated RAW264.7 cells were used as the in vitro model to validate the modulating effects of FHD on molecules/inflammatory mediators using various biomedical techniques/kits such as MTT assay, Griess reagents, flow cytometry, RT-qPCR, and immunoblotting. Network pharmacology analyses indicated a total of 20 major active components and 30 core biological targets of FHD against RA. Pathway enrichment analyses demonstrated the involvement of mitogen-activated protein kinase (MAPK) signaling pathways in the efficacy of the formula. Furthermore, experimental evidence demonstrated that FHD dose-dependently and significantly inhibited the productions of nitric oxide (NO) and reactive oxygen species; lowered the mRNA expression levels of proinflammatory mediators including iNOS, COX-2, TNF-α, IL-1β, and IL-6; decreased protein levels of the phosphorylated forms of p38, ERK, JNK, and NF-κB p65. Additionally, the results of molecular docking showed that tetrandrine, licochalcone A, oxonantenine, isorhamnetin, and kaempferol in FHD exerted the potent capability of binding to target molecules in the focused signaling pathway, probably being the potential effective substances for FHD. Our network pharmacology study integrated with cellular validation has elucidated that FHD exerts downregulating effects of the MAPK and NF-κB signaling pathway, ultimately leading to inhibitory effects on the productions of proinflammatory mediators in LPS-stimulated RAW264.7 cells. This work comprehensively demonstrated the effective substances, key targets, and signaling pathways involved in the anti-RA effects of the formula, and these findings provide a further understanding of the underlying mechanism of FHD in managing RA.

1. INTRODUCTION

The prevalence of rheumatoid arthritis (RA) worldwide ranges from 0.5 to 1%, with females and the elderly comprising the majority.[1] The main pathological features of RA are primarily distinguished by the extensive presence of inflammatory cells, along with the abnormal growth of synovial cells and the development of pannus.[2] These pathological processes lead to severe erosion of cartilage and bone, resulting in destruction and deformity of joint structures, ultimately leading to complete loss of joint function.[3] Currently, the widely used therapeutic agents for RA include three types: glucocorticoids, nonsteroidal anti-inflammatory drugs (NSAIDS), and disease-modifying anti-rheumatic drugs (DMARDs).[4] DMARDs encompass conventional synthetic agents, biological therapeutics, biosimilar products, and targeted synthetic compounds.[5] Methotrexate (MTX), a leading DMARD, has been extensively utilized clinically for the treatment of RA.[6,7] These drugs have received widespread attention and restrictions due to the presence of severe adverse effects, as well as the escalating risks of gastric mucosa damage, metabolic disorders, and osteoporosis, yet their therapeutic effects remain unsatisfactory.[6−8] Chinese medicines have been widely accepted for their remarkable therapeutic effect and low toxicity.[9,10] Accordingly, exploring drugs from traditional Chinese medicine (TCM) classics is a practical and effective approach for treating RA.

Fangji Huangqi decoction (FHD for short) was first documented in the TCM classic work Jin Gui Yao Lue, which was authored by the renowned medical expert Zhang Zhongjing and published more than 1800 years ago.[11] This formula is known for its effectiveness in augmenting Qi, raising Yang, promoting urination, and reducing swelling.[12] In clinical practice, FHD is often used to treat conditions such as rheumatism, joint pain, edema, beriberi, frequent urination, and eczema.[13] As documented, FHD consists of four herbs, namely, *Stephaniae tetrandrae* Radix (STR for short, *Fangji* in Chinese), *Astragali* Radix (AR for short, *Huangqi* in Chinese), *Atractylodis macrocephalae* Rhizoma (AMR for short, *Baizhu* in

Received: April 11, 2024
Revised: June 24, 2024
Accepted: June 26, 2024
Published: July 10, 2024

Chinese), and *Glycyrrhizae* Radix (GR for short, *Gancao* in Chinese).[14] The main components of FHD include alkaloids (e.g., tetrandrine and fangchinoline) and flavonoids (e.g., astragaloside and glycyrrhizic acid).[15] Studies have shown that FHD could significantly improve the degree of foot swelling in collagen-induced arthritis rat models by modulating the PI3K/AKT and Notch2/DLL1 signaling pathways and inhibiting the production of inflammatory factors.[16,17] An increasing number of studies have reported that compounds occurring in FHD including resveratrol, tetrandrine, and kaempferol possess potent anti-inflammatory activities, and chemicals of tetrandrine and fangchinoline occurring in FHD had been reported to exert inhibitory effects of activation of the mitogen-activated protein kinase (MAPK)/NF-κB signaling pathways.[18−23] However, the key mechanism of action of FHD in treating RA and whether the MAPK/NF-κB signaling pathways are involved in the effects of the formula remain obscure.

In this work, HPLC technology was used for quality control of FHD, and the underlying mechanism of FHD against RA was explored using approaches including network pharmacology, molecular docking, and in vitro experiments. The findings of this work provide a further understanding of the underlying mechanism of FHD against RA.

2. MATERIALS AND METHODS

2.1. Materials. Phosphate-buffered saline (PBS), fetal bovine serum, and Dulbecco's modified Eagle's medium were purchased from Biological Industries (Kibbutz, Israel). Lipopolysaccharide (LPS), BCA Assay Kit, and MTT were purchased from Beijing Solarbio (Beijing, China). Fangchinoline, tetrandrine, calycosin 7-*o*-glucoside, liquiritin, and glycyrrhizic acid were purchased from Chengdu PureChem-Standard Co., Ltd. (Chengdu, China). p38, p-p38, ERK, p-ERK, SAPK/JNK, p-SAPK/JNK, NF-κB p65, and p-NF-κB p65 were purchased from Cell Signaling Technology Beverly (Massachusetts, USA). RAW264.7 cells were procured from ATCC.

2.2. Preparation of Extract. A total of four herbs in FHD including STR, AR, GR, and AMR were obtained from Zhang Zhongjing Pharmacy, in Zhengzhou, China. These herbs were further authenticated by the corresponding author, Professor Dai Liping, as originating from *Stephania tetrandra* S.Moore, *Astragalus membranaceus* Fisch, *Glycyrrhiza uralensis* Fisch., and *Atractylodes macrocephala* Koidz., respectively. A voucher specimen bearing the identification number 20220725 was deposited at the Henan Provincial Laboratory for Comprehensive Development and Utilization of Authentic Medicinal Materials, Henan University of Chinese Medicine, to ensure its long-term preservation. To prepare the aqueous extract of the formula, STR (12 g), AR (15 g), GR (6 g), and AMR (9 g) were immersed separately in 10 times their mass in water for 30 min and then heated to boiling for 1 h. Subsequently, the liquid was separated from the herbs. For the second decoction, another 10 times the mass of water was added and boiled for another hour. The resulting concentrate was then freeze-dried to obtain powder, with a yield of 9.7% for FHD.

2.3. HPLC Analyses. In pharmacological research, quality control is crucial to ensure the safety, efficacy, and consistency of the extract/drug, thereby enabling reliable scientific evaluation and therapeutic application. HPLC, as an efficient and accurate analytical technique, plays a crucial role in quality control and analysis of active ingredients in natural products.[24,25] Accordingly, an HPLC system (Shimadzu, Japan) was used to quantify the content of FHD freeze-dried powder for quality control. Chromatographic separation was achieved on a Shimpack GIST column (4.6 mm, 250 mm, 5 μm) maintained at 30 °C, with a PAD detector set to detect wavelengths spanning from 190 to 400 nm. The mobile phase comprised acetonitrile (A) and a 0.1% phosphoric acid solution (B). The separation process is shown in Table 1.[26]

Table 1. Chromatographic Conditions

time	organic phase	aqueous phase
0	5	95
10	10	90
15	16	84
35	16	84
40	23	77
43	23	77
53	25	75
55	27	73
60	29	71
65	38	62
80	38	62
85	5	95
93	5	95

2.4. Collection of Active Chemicals in FHD. The TCM System Pharmacology (TCMSP) database was used to get compounds of FHD, the OB 30% and OL 0.18 were filter criteria. For additional information, known FHD active ingredients were collected using the Swiss ADME platform, and the acquired compound targets were tracked. The criteria for selecting potential core compounds and targets included a "high" gastrointestinal absorption (GIabsorption) rating, as well as satisfying two or more "yes" outcomes across five categories of pharmacological prediction (Lipinski, Ghose, Veber, Egan, and Muegge).

2.5. Acquisition of FHD Target Genes. Human genes associated with RA were retrieved from three databases, namely the GeneCards, OMIM, and TTD databases. The merged data sets were then deduplicated. Subsequently, the active ingredient targets and RA targets were visualized in a Venn diagram using online drawing tools available at Bioinformatics (https://www.bioinformatics.com.cn/).

2.6. Construction of a Protein−Protein Interaction (PPI) Network of Common Targets of FHD and RA. The STRING11.0 database (http://string-db.org) contains the gene targets mentioned previously with "*Homo sapiens*" specified as the species. A threshold score exceeding 0.40 was utilized to extract the PPI network. The generated network was saved as a TSV file and then imported into Cytoscape version 3.10.0 for visualization.

2.7. Gene Ontology (GO) and Kyoto Encyclopedia of Gene and Genome (KEGG) Analyses. The examination of the GO categories encompasses cellular components (CCs), biological processes (BPs), and molecular functions (MFs). Besides, the KEGG pathways associated with FHD in relation to RA were conducted on the intersection targets of drug-disease using the Metascape web platform.

2.8. Molecular Docking. The chemical structures in SDF format were obtained from the PubChem database and then imported into the ChemDraw 3D software for further analysis. Energy minimization was conducted utilizing the MM2 module to attain the conformation with the minimum energy, which was then saved in the form of a mol2 file. Protein structures

https://doi.org/10.1021/acsomega.4c03495
ACS Omega 2024, 9, 31878−31889

Table 2. Primer of Inflammation Factors for Mouse

primer name	forward primer (5′-3′)	reverse primer (5′-3′)
iNOS	TCACTCAGCCAAGCCCTCAC	TCCAATCTCTGCCTATCCGTCTC
COX-2	GTGCCTGGTCTGATGATGTATGC	TGAGTCTGCTGGTTTGGAATAGTTG
IL-6	CTCCCAACAGACCTGTCTATAC	CCATTGCACAACTCTTTTCTCA
IL-1β	CACTACAGGCTCCGAGATGAACAAC	TGTCGTTGCTTGGTTCTCCTTGTAC
TNF-α	ATGTCTCAGCCTCTTCTCATTC	GCTTGTCACTCGAATTTTGAGA
β-actin	TGCAGTTGCTTTATTCTCCCAT	TGTTGCCACGCCTTCATTC

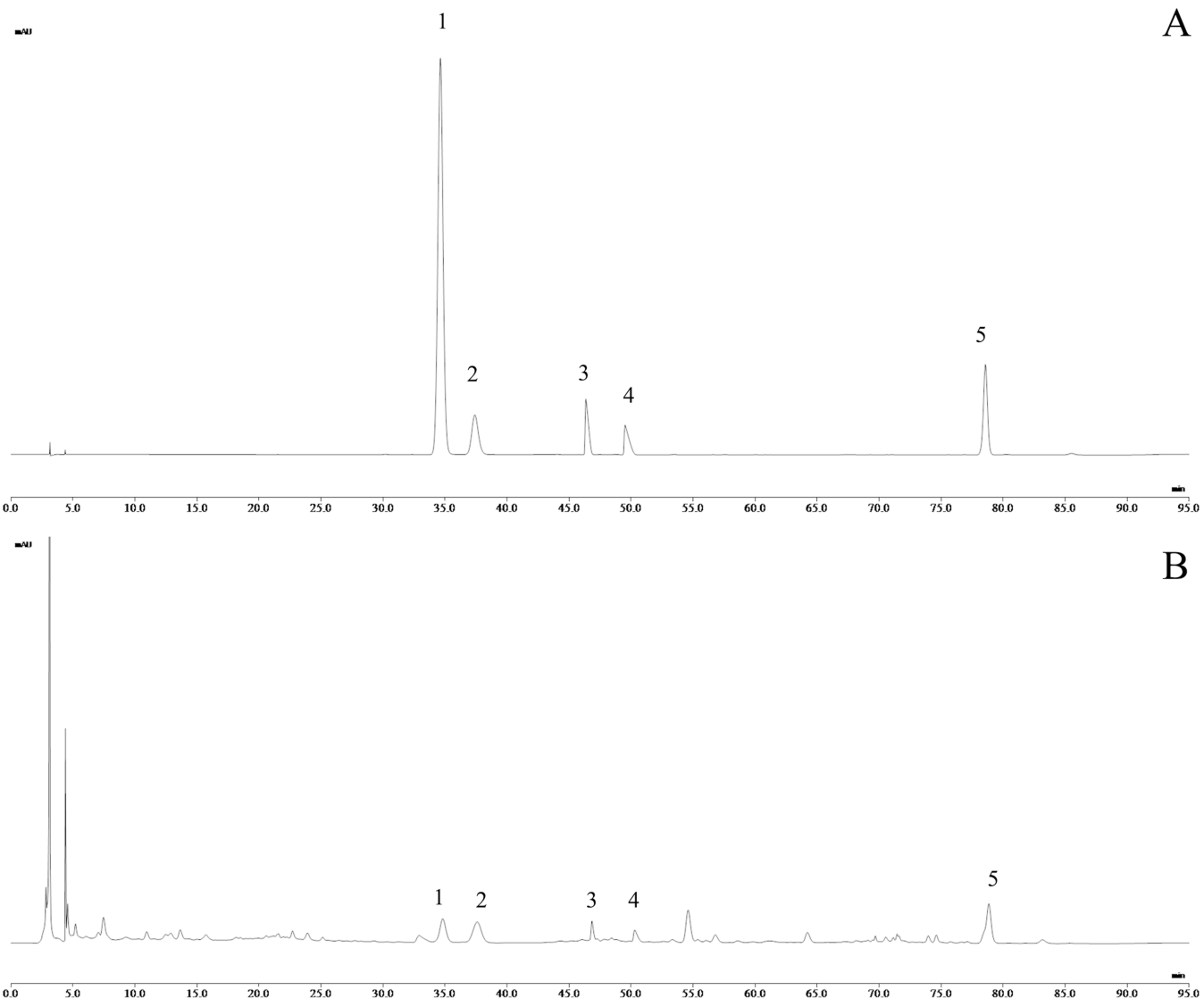

Figure 1. HPLC chromatogram of sample and mixed reference substances. (A) Mixed standards. (B) FHD [(1) liquiritin; (2) calycosin 7-*o*-glucoside; (3) fangchinoline; (4) tetrandrine; (5) glycyrrhizic acid].

associated with MAPK/NF-κB signaling pathways (MAPK1, JNK3, JUN, p38, MAPK3, ERK, and p65) were obtained from the Protein Data Bank (PDB) database. Following this, Discovery Studio was utilized for dehydration, hydrogenation, charge calculation, and the amalgamation of nonpolar hydrogen atoms. The ligands and receptors were stored separately. Optimization of the candidate compound structures was conducted prior to initiating the docking experiment.

2.9. MTT Assay. RAW 264.7 cells were cultured as previously described. Five $\times 10^4$ cells/mL RAW 264.7 cells were seeded in 96-well plates and exposed to different concentrations of FHD in absence or presence of LPS (2 μg/mL) for 24 h. Following treatment, 20 μL of MTT was added, the culture medium was aspirated, and DMSO was added after 4 h. Absorbance values at 490 nm were measured using a spectrophotometer (Thermo, CHN), and cell viability (%) was subsequently calculated.

2.10. NO Assay. A density of 2×10^5 cells/mL RAW264.7 cells were incubated in 24-well plates for 24 h. Subsequently, they were subjected to FHD at indicated concentration for 30 min and then stimulated with 2 μg/mL LPS for another 24 h. Following treatment, the supernatant of cells was assessed for nitric oxide (NO) content using the Griess reagent, and the NO

https://doi.org/10.1021/acsomega.4c03495
ACS Omega 2024, 9, 31878−31889

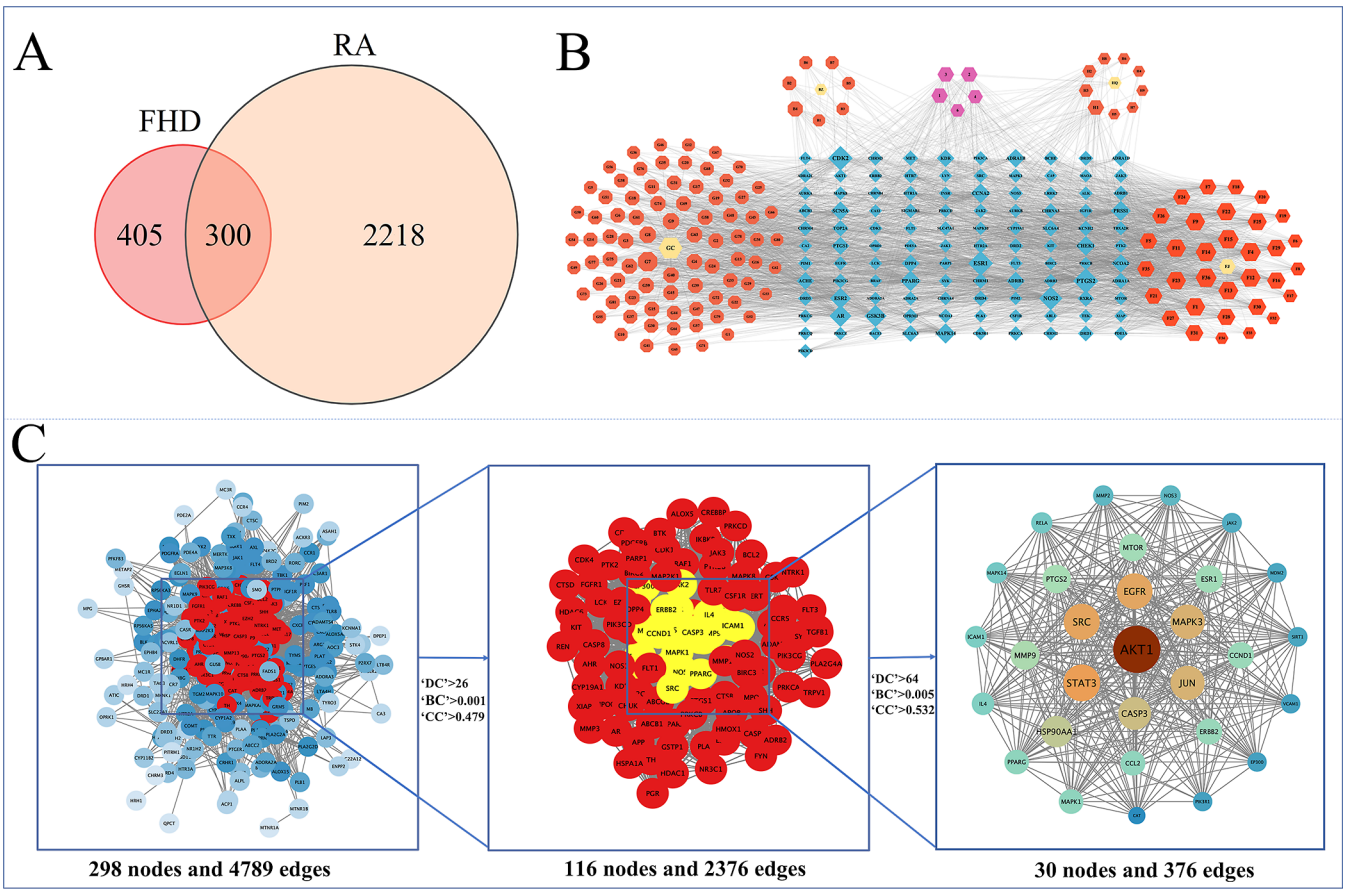

Figure 2. Results of network pharmacology analyses of FHD against RA. (A) Venn diagram of FHD and RA targets. (B) FHD-component-target network. The Chinese medicines are depicted as yellow rectangle nodes, their compounds as red ellipse nodes, and the disease genes as blue polygon nodes. (C) Core targets of the PPI network.

levels for each experimental group were quantified utilizing a standard curve developed using the standard of $NaNO_2$.

2.11. Real-Time PCR Analysis. Cells were collected, and total RNA was extracted using TRIzolTM, and total RNA was transcribed into cDNA by Superscript III RT-qPCR Kit (Serbicebio, CHINA). Reverse transcription-quantitative PCR (RT-qPCR) was then performed on the cDNA by SYBR GREEN (Monad, CHINA). The primer sequences are shown in Table 2.

2.12. Reactive Oxygen Species (ROS) Levels. Quantification of ROS production was conducted with the 2′,7′-dichlorofluorescein diacetate (DCFH-DA) fluorescent probe as per the manufacturer's instructions. In detail, 1 mL of DCFH-DA diluted at a ratio of 1:1000 was introduced, and the cells were then incubated for 30 min. Afterward, the cells were rinsed twice with PBS. Subsequently, cell morphology and ROS fluorescence levels were examined using the Olympus IX73 inverted fluorescence microscope, with analysis conducted utilizing ImageJ 1.8.0. Additionally, ROS levels were assessed using the BD Accuri C6 Plus Flow Cytometer and analyzed using FlowJO software.

2.13. Western Blot. The proteins of cells were extracted according to previously described methods. Equivalent quantities of protein extracts (30 μg) were separated by electrophoresis on 10% SDS-polyacrylamide gels and then transferred to PVDF membranes. Primary antibody dilutions were prepared as follows: p38, p-p38, ERK, p-ERK, p65, p-p65, SAPK/JNK and p-SAPK/JNK, β-actin (1:1000 dilution). The secondary antibody used was goat antirabbit IgG conjugated at a dilution of 1:10,000. Images were captured using the Tanon 5200 Multi fully automatic chemiluminescence imaging analysis system, with subsequent grayscale value detection and analysis performed using ImageJ 1.8.0.

2.14. Statistical Analysis. Statistical analysis was performed with GraphPad Prism 9.5.0 (GraphPad Software, CA, USA). Mean differences were evaluated through one-way analysis of variance coupled with the Bonferroni multiple comparison test. Statistical significance was established at $p < 0.05$.

3. RESULTS

3.1. FHD Content Determination. The injection volume for each sample was 15 μL. The concentrations of five chemical substances including fangchinoline, tetrandrine, calycosin 7-o-glucoside, liquiritin, glycyrrhizic acid, in FHD were 7.63, 1.12, 1.93, 7.87, and 11.97%, respectively (Figure 1).

3.2. Network Pharmacology-Based Analysis. *3.2.1. Active Chemical Compositions and Target Prediction of FHD.* A total of 148 compounds were obtained about FHD from TCMSP and Swiss ADME platforms. After normalization in UniProt (http://www.uniprot.org/), 705 targets related to 148 compounds were screened.

3.2.2. Prediction of RA Targets. A cumulative count of 5038 gene targets associated with "Rheumatoid arthritis" keywords was compiled from the OMIM, TTD, and GeneCards databases, with redundant genes removed to establish the RA target set.

https://doi.org/10.1021/acsomega.4c03495
ACS Omega 2024, 9, 31878−31889

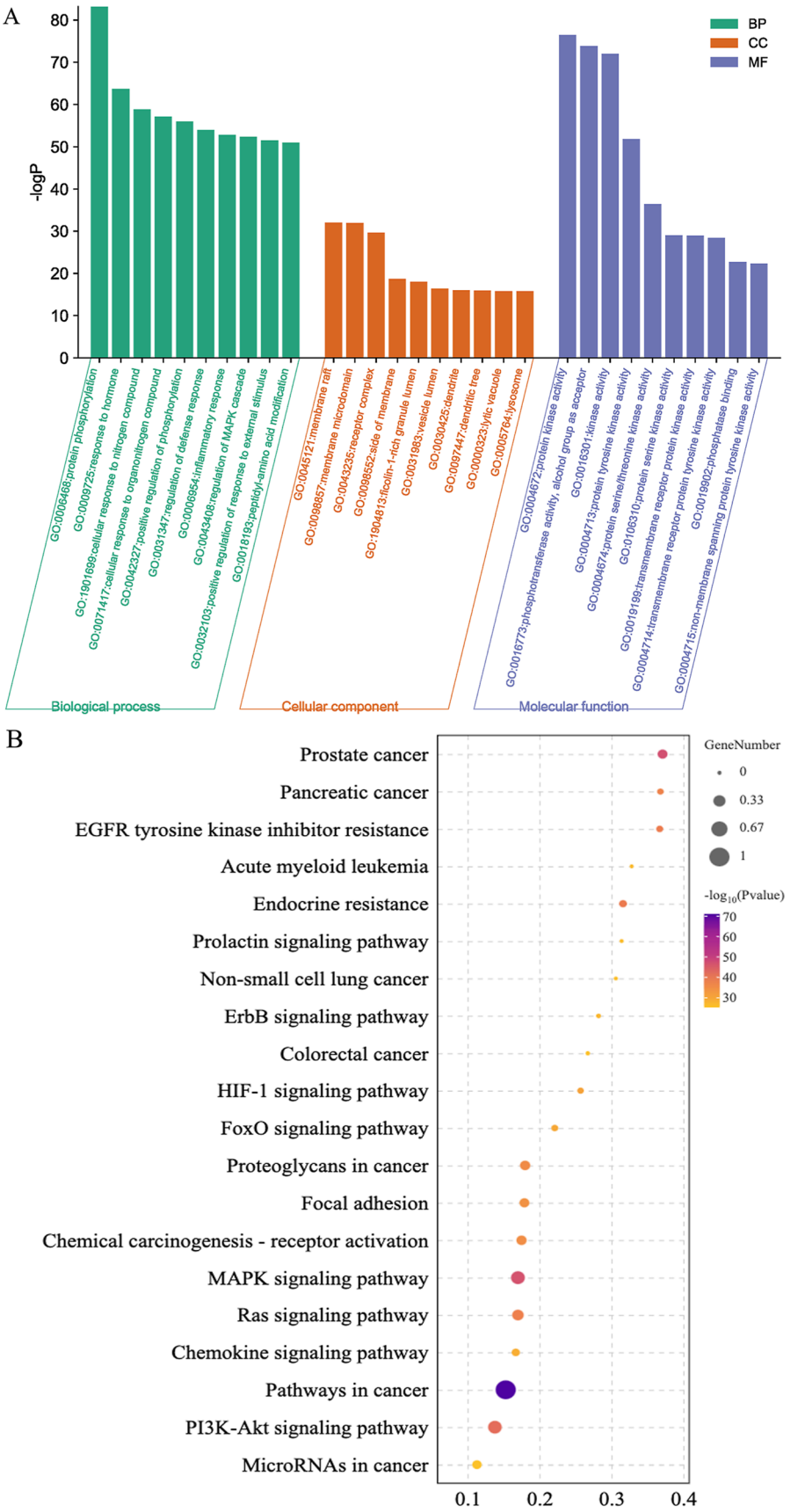

Figure 3. GO and KEGG analyses. (A) GO enrichment analysis of 300 targets. (B) KEGG pathway enrichment analysis of the top 20.

https://doi.org/10.1021/acsomega.4c03495
ACS Omega 2024, 9, 31878−31889

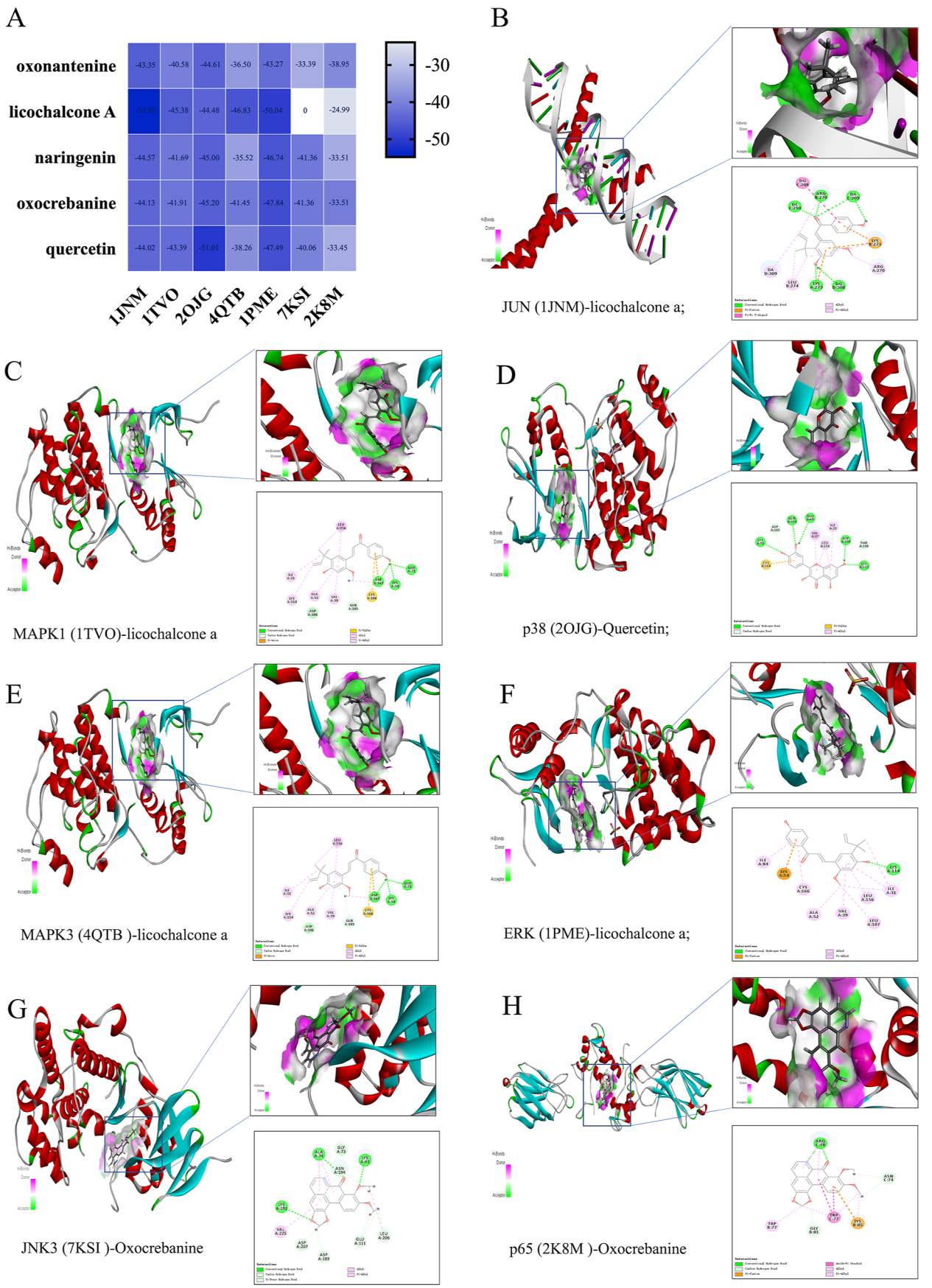

Figure 4. Results of molecular docking. (A) Binding energy of the main active components of FHD and the key protein targets. (B−H) Binding site of the main active components of FHD and the key targets. (B) JUN (1JNM)-licochalcone A. (C) MAPK1 (1TVO)-licochalcone A. (D) p38 (2OJG)-quercetin. (E) MAPK3 (4QTB)-licochalcone A. (F) ERK (1PME)-licochalcone A. (G) JNK3 (7KSI)-oxocrebanine. (H) p65 (2K8M)-oxocrebanine.

https://doi.org/10.1021/acsomega.4c03495
ACS Omega 2024, 9, 31878−31889

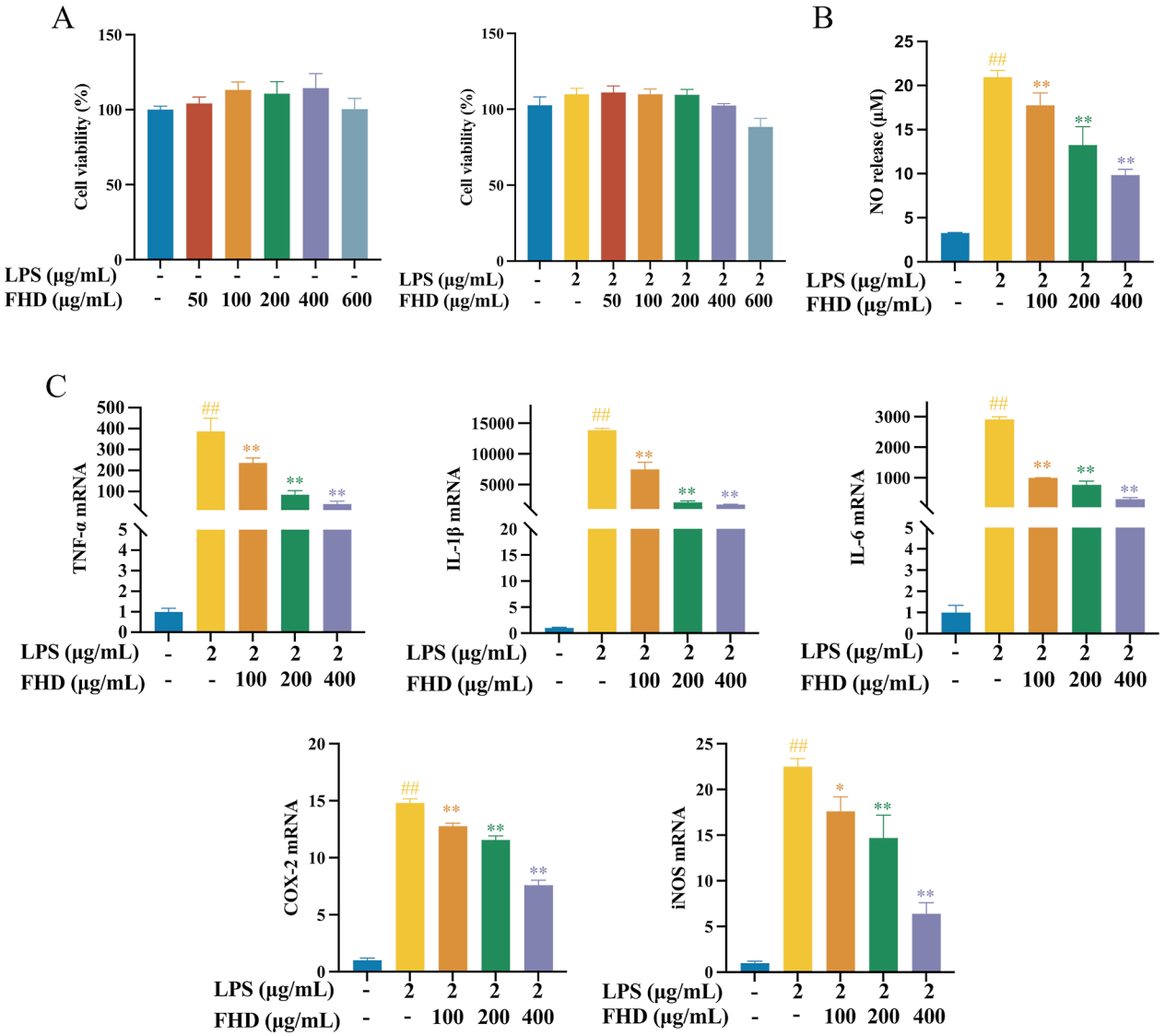

Figure 5. FHD significantly inhibited the production of proinflammatory mediators in LPS-stimulated RAW264.7 cells. (A) Effects of FHD on the RAW264.7 cells' viability in the absence (left panel) or presence (right panel) of LPS (2 μg/mL). (B) NO release. (C) mRNA expression levels of proinflammatory factors. Results are expressed as the mean ± SD (n = 3), *P < 0.05, **P < 0.01 vs. model group, $^{\#\#}P$ < 0.01 vs. control group.

Subsequently, applying a filter based on twice-median relevance scores between diseases and targets, a subset of 2519 targets were identified as pertinent to the disease.

3.2.3. PPI Network of FHD and RA Common Targets. Venn diagrams highlighted an intersection of 300 genes between the corresponding targets of FHD and RA (Figure 2A). To visually depict the relationship between drug ingredients and disease targets, an FHD-ingredient-targets-RA network diagram was constructed (Figure 2B). The 300 gene targets were utilized to generate a PPI network through the STRING database and software of Cytoscape. Employing the Maximum Clique Centrality, a recent network topology algorithm integrated into CytoNCA, we identified 30 core targets, including MAPK1, MAPK3, JUN, and others (Figure 2C).

3.2.4. GO and KEGG Analyses. Enrichment analysis of KEGG and GO was conducted with Metascape (http://metascape.org/), and the top 10 pathways was selected based on $Log^{10}(P)$ values. GO enrichment analysis of the intersectional targets encompassed the BP, CC, and MF. Regarding the BP, the intersectional targets exhibited enrichment in the regulation of the MAPK cascade, protein phosphorylation, modulation of the defense response, inflammatory response, and positive modulation of response to external stimuli. Concerning the CC, enrichment was observed in membrane rafts, membrane microregions, and intravascular lumen. For MF, enrichment was evident in protein kinase activity, protein tyrosine kinase activity, kinase activity, and phosphatase binding (Figure 3A). The KEGG pathways involved included cancer pathways, MAPK signaling pathway, EGFR tyrosine kinase inhibitor resistance, PI3K-Akt signaling pathway, alongside other pathways (Figure 3B).

3.2.5. Molecular Docking. The MAPK signaling pathway as well as NF-κB signaling pathway-related targets 1JNM (JUN), 1TVO (MAPK1), 2OJG (p38), 4QTB (MAPK3), 1PME (ERK), 7KSI (JNK3), and 2K8M (p65) identified by KEGG were aligned with compounds in the top five of the degree values (licochalcone A, oxonantenine, naringenin, oxocrebanine, and quercetin). The molecular docking technique was employed to estimate the binding energy between the ligand (compound) and the receptor (protein), as depicted in Figure 4. The results

https://doi.org/10.1021/acsomega.4c03495
ACS Omega 2024, 9, 31878−31889

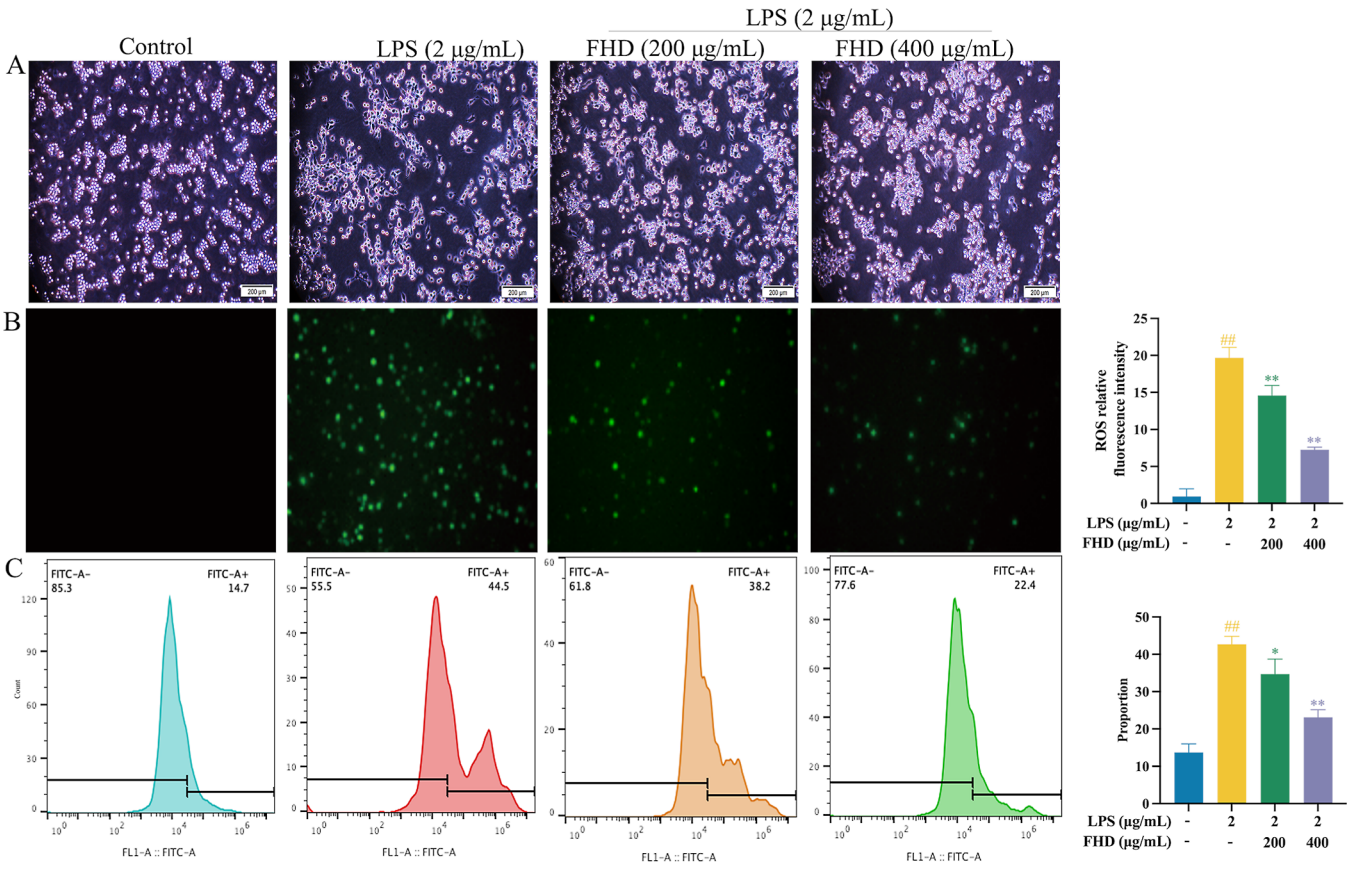

Figure 6. FHD inhibited the production of ROS in LPS-induced RAW264.7 macrophages. (A) Effects of FHD on cell morphology. (B) Fluorescence microscopy imaging. (C) Flow cytometry analyses. Results are expressed as the mean ± SD ($n = 3$), *$P < 0.05$, **$P < 0.01$ vs. model group, $^{\#\#}P < 0.01$ vs. control group.

showed that licochalcone A has strong binding affinities with JUN, MAPK1, and MAPK3, which were −54.79, −45.38, and −46.83, respectively. Quercetin indicated a binding affinity of −51.01 with p38, while oxocrebanine showed binding affinities of −40.83 and −41.52 with p65 and JNK, respectively. The binding free energy derived from molecular docking serves as a critical parameter for assessing the stability of drug−target interactions, whereby a lower binding free energy value indicates a more stable binding of the drug to the target.

3.2.6. FHD Inhibited the Release of Inflammatory Cytokines. As illustrated in the left panel of Figure 5A, FHD exhibited no cytotoxic effects within the concentration ranging from 50 to 600 μg/mL, maintaining cell viability above 90%. In the right panel of Figure 5A, cells were pretreated with various concentrations (50−600 μg/mL) of FHD for 30 min before the induction of LPS (2 μg/mL) in RAW264.7 cells. After 24 h, MTT assay was conducted. Results indicated that cell viability remained consistently above 90% ranging from 50 to 600 μg/mL of FHD. Consequently, the concentrations of 200 and 400 μg/mL were selected for subsequent experiments. As depicted in Figure 5B, Griess assay was used to detect the effect of FHD on the secretion of NO in LPS-induced RAW264.7 cells. Notably, FHD intervention significantly reduced NO release in the cell supernatant of LPS-induced RAW264.7 cells. As demonstrated in Figure 5C, RT-qPCR was used to detect the inhibitory effects of FHD on mRNA expression levels of inflammation-related genes in LPS-induced RAW264.7 cells. As our result indicated, LPS induction significantly upregulated mRNA expression levels of inflammation-related genes COX-2, TNF-α, iNOS, IL-1β, and IL-6. And, FHD treatment decreased the expression levels of these inflammation-related genes in a concentration-dependent manner.

3.2.7. FHD Inhibited the Release of ROS. To determine whether FHD could influence ROS release, LPS-induced RAW264.7 cells were pretreated with various concentrations of FHD for 4 h. It was observed that FHD markedly inhibited cell differentiation and reduced pseudopodia in a concentration-dependent manner, when compared with those in the group with single LPS induction (Figure 6A). After FHD treatment, the cells were stained with DCFH-DA and were subsequently observed with a flow cytometer. As shown, the release of ROS was increased in the LPS-induced RAW264.7 cell group compared to those in the control group. However, pretreatment with FHD effectively inhibited the release of ROS under LPS stimulation conditions (Figure 6C). Photos were taken at the same laser intensity using laser scanning confocal microscopy, observing an increase in green fluorescence in the areas of LPS stimulation, whereas FHD pretreatment decreased the green fluorescence (Figure 6B). The results of flow cytometry and laser scanning confocal microscopy indicated that FHD could effectively inhibit the release of ROS in LPS-induced RAW264.7 cells.

3.2.8. FHD Inhibited the Activation of the MAPK/NF-κB Signaling Pathways. Western blot analysis was performed to evaluate the impact of FHD on the inhibition of MAPK and NF-κB phosphorylation signaling pathways (Figure 7). Results revealed that the increase on protein levels of phosphorylated form of p38, ERK, JNK, and NF-κB were induced by LPS in

https://doi.org/10.1021/acsomega.4c03495
ACS Omega 2024, 9, 31878−31889

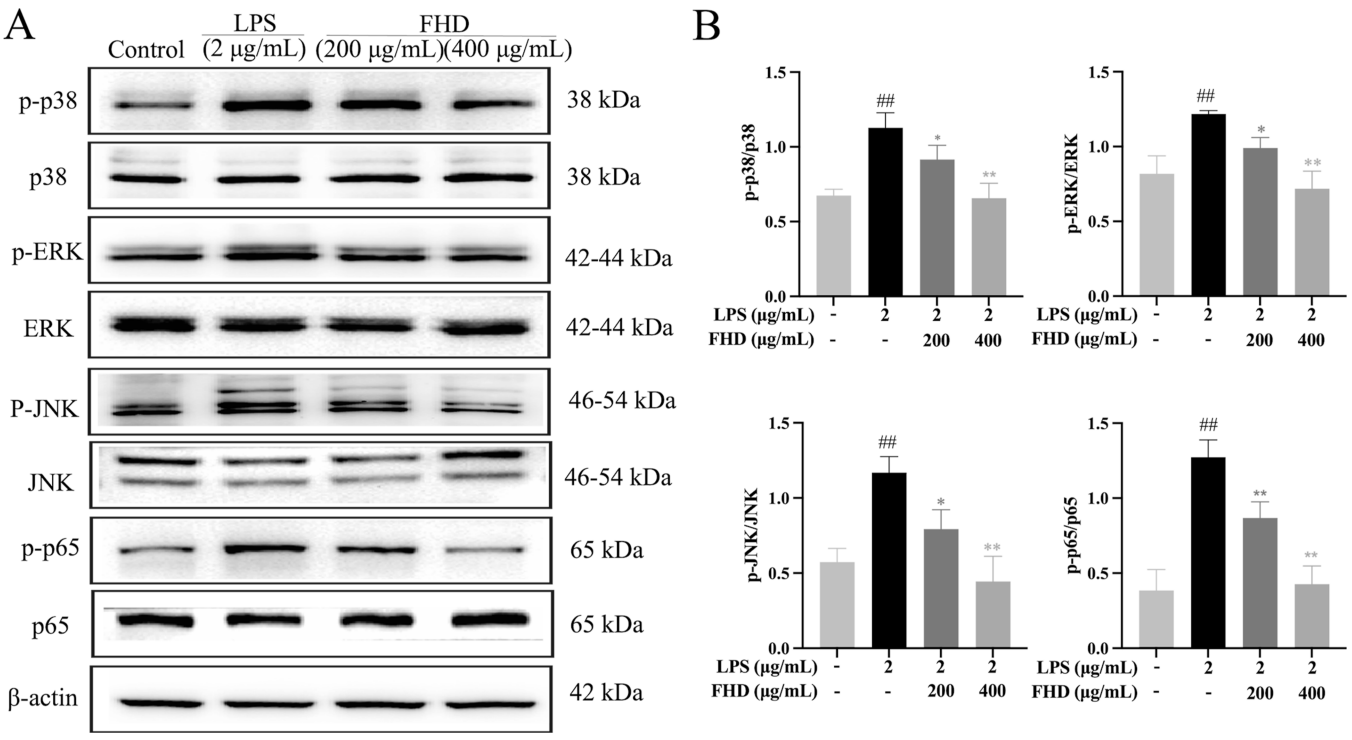

Figure 7. FHD inhibited the phosphorylation/activation of molecules in the MAPK/NF-κB signaling pathway in LPS-induced RAW264.7 cells. (A) Western blotting was employed to analyze the representative images of phosphorylated and nonphosphorylated forms of p38, ERK, JNK, and NF-κB p65 in cells. (B) Densitometric values were normalized to those of the control group. Results are presented as the mean ± standard deviation ($n = 3$), $^{*}P < 0.05$, $^{**}P < 0.01$ vs. group treated with single LPS (2 μg/mL), $^{\#\#}P < 0.01$ vs. control group.

RAW264.7 cells. Afterward, FHD significantly decreased the protein levels of phosphorylated form of p38, ERK, JNK, and NF-κB in a concentration-dependent manner.

4. DISCUSSION

RA is a chronic autoimmune disease characterized by inflammation of the synovium, cartilage erosion, and bone tissue damage in the joints, ultimately leading to joint deformity and loss of function.[1] Studies have demonstrated that the TCM formula of FHD may be an effective agent for treating RA.[27−29] Our research employed network pharmacology, molecular docking, and in vitro experimental validation to elucidate the underlying mechanisms of FHD against RA.

In recent years, the network pharmacology method has been approved as a discipline that utilizes network analysis and systems biology methods to investigate the mechanisms of drug and drug−drug interactions, which have been widely applied in the field of TCM research.[30,31] In terms of mechanistic elucidation on FHD-RA interaction, as shown in Figure 3, essential associated functions were identified through GO enrichment analysis originating from 300 intersecting genes related to the pathogenesis of RA, including protein phosphorylation, inflammatory response, and positive regulation of response to external stimuli. As indicated in PPI network analyses, genes such as JUN, MAPK3, and MAPK1 could play crucial roles in the pathogenesis of RA as they are key targets in the MAPK signaling pathway. Meanwhile, results of KEGG analyses indicated that the MAPK signaling pathway could be implicated in the effects of the formula when treating RA, which was consistent with the findings of the PPI analyses as indicated previously. Accumulating mechanistic studies have demonstrated that RA is a chronic inflammatory disease characterized by the activation of the MAPKs, including ERK, JNK, and p38, which is instrumental in the activation of nuclear factor κ-B NF-κB, a protein complex that controls transcription of DNA, cytokine production, and cell survival functions.[32,33] Once activated, the NF-κB phosphorylates and activates the inhibitory κ-B kinase complex, leading to the degradation of Iκ-B and the subsequent release and nuclear translocation of NF-κB.[34] Abnormally elevated MAPK signaling pathway activity could promote the release of proinflammatory mediators including TNF-α, IL-6, IL-1β, NO, iNOS, and COX-2, leading to joint tissue damage and impairment of joint function, exacerbating the pathological process of arthritis and worsening symptoms such as joint pain, swelling, and functional impairment in patients.[35−38]

Macrophages play a pivotal role in inflammation-related studies and the inflammatory process in RA.[39] These cells, abundant in the synovium and cartilage vasculature, produce proinflammatory cytokines and chemokines in response to external factors like LPS, driving RA progression.[36,40,41] Therefore, LPS-induced macrophages were used as an in vitro model to investigate the molecular mechanism of FHD against RA in the present work. Oxidative stress, a key factor in RA pathogenesis, occurs when ROS production exceeds the cellular antioxidant capacity, exacerbating inflammation and activating the NF-κB signaling pathway.[42,43] Previous studies have demonstrated and reported the antioxidant and anti-inflammatory effects of compounds in FHD, including tetrandrine, isorhamnetin, and licochalcone A.[44−46] Our result showed that FHD could significantly inhibit ROS release in LPS-stimulated macrophages. Furthermore, LPS-induced RAW264.7 cells significantly increased the mRNA levels of TNF-α, IL-1β, IL-6, iNOS, COX-2, and ROS, as well as the protein levels of phosphorylated proteins in the MAPK and NF-κB signaling

https://doi.org/10.1021/acsomega.4c03495
ACS Omega 2024, 9, 31878−31889

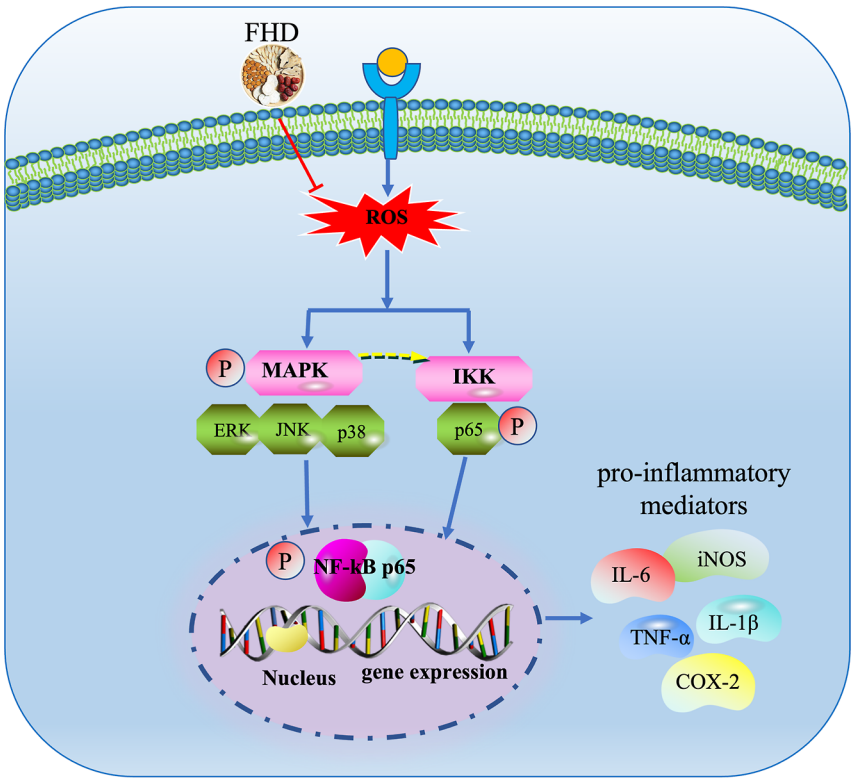

Figure 8. Anti-RA effects of FHD involve inhibition of MAPK and NF-κB signaling pathways.

pathways. Notably, FHD effectively inhibited the expression of these phosphorylated proteins and the production of inflammatory factors, suggesting the involvement of the MAPK and NF-κB signaling pathways in the effects of FHD against RA.

In addition, molecular docking is a powerful tool for virtual screening and understanding potential molecular interactions and could be used as a starting point for drug discovery. As our docking results indicated, each indicted target/molecule related to the MAPK and NF-κB signaling pathways exerted potent binding affinity with the flavonoids (e.g., licochalcone A and quercetin), as well as alkaloids (e.g., oxocrebanine), which were probably the potential effective substances in FHD.

This work aims to investigate the molecular mechanism underlying the anti-RA effects of FHD, using approaches including network pharmacology, computational models, and experimental validation in vitro. However, it is an inevitable challenge for this work that the obtained data could not fully capture the complexity of in vivo biological systems. Accordingly, studies in vivo are warranted to investigate the effective substance/fraction and involvement of focused signaling pathways in the therapeutic effects of FHD.

5. CONCLUSIONS

Our network pharmacology study integrated with cellular validation has elucidated that FHD exerts the downregulating effects of the MAPK and NF-κB signaling pathways, ultimately leading to inhibitory effects on productions of proinflammatory mediators in LPS-stimulated RAW264.7 cells (Figure 8). This work comprehensively demonstrated the effective substances, key targets, and signaling pathways involved in anti-RA effects of the formula, and these findings provide a further understanding of the underlying mechanism of FHD in managing RA.

AUTHOR INFORMATION

Corresponding Author

Liping Dai − *Collaborative Innovation Center of Research and Development on the Whole Industry Chain of Yu-Yao, Henan University of Chinese Medicine (HUCM), Zhengzhou, Henan 450000, China; School of Pharmacy, HUCM, Zhengzhou, Henan 450000, China;* orcid.org/0009-0003-0240-8763; Email: liping_dai@hactcm.edu.cn

Authors

Weijin Zhang − *Collaborative Innovation Center of Research and Development on the Whole Industry Chain of Yu-Yao, Henan University of Chinese Medicine (HUCM), Zhengzhou, Henan 450000, China; School of Pharmacy, HUCM, Zhengzhou, Henan 450000, China*

Hui Guo − *Collaborative Innovation Center of Research and Development on the Whole Industry Chain of Yu-Yao, Henan University of Chinese Medicine (HUCM), Zhengzhou, Henan 450000, China; School of Pharmacy, HUCM, Zhengzhou, Henan 450000, China*

Leyuan Li − *Collaborative Innovation Center of Research and Development on the Whole Industry Chain of Yu-Yao, Henan University of Chinese Medicine (HUCM), Zhengzhou, Henan 450000, China; School of Pharmacy, HUCM, Zhengzhou, Henan 450000, China*

Mengmeng Zhang − *Collaborative Innovation Center of Research and Development on the Whole Industry Chain of Yu-Yao, Henan University of Chinese Medicine (HUCM), Zhengzhou, Henan 450000, China; School of Pharmacy, HUCM, Zhengzhou, Henan 450000, China*

Erping Xu − *Collaborative Innovation Center of Research and Development on the Whole Industry Chain of Yu-Yao, Henan University of Chinese Medicine (HUCM), Zhengzhou, Henan 450000, China*

https://doi.org/10.1021/acsomega.4c03495
ACS Omega 2024, 9, 31878−31889

Complete contact information is available at:
https://pubs.acs.org/10.1021/acsomega.4c03495

Author Contributions

[§]W.Z. and H.G. contributed equally to this work. W.Z. and H.G. proposed the ideas, designed the experiments, and wrote the manuscript. L.L. and M.Z. analyzed the data; L. D. and E.X. designed and supervised the study.

Notes

The authors declare no competing financial interest.

■ ACKNOWLEDGMENTS

This work was supported by the Joint Fund of Science and Technology Research and Development Plan of Henan Province (no. 222301420082), the Provincial Key Technologies R&D Program of Henan Province (no.221100310400), the Key Research Project on Traditional Chinese Medicine Culture and Management of Henan (no. TCM2021013), and the National Key Research and Development Program of China (2023YFC3504000).

■ REFERENCES

(1) Zamudio Cuevas, Y.; Martínez Flores, K.; Martínez Nava, G. A.; Clavijo Cornejo, D.; Fernández Torres, J.; Sánchez, R. Rheumatoid arthritis and oxidative stress, a review of a decade. *Cell. Mol. Biol.* **2022**, *68* (6), 174−184.

(2) Deloch, L.; Fuchs, J.; Ruckert, M.; Fietkau, R.; Frey, B.; Gaipl, U. S. Low-Dose Irradiation Differentially Impacts Macrophage Phenotype in Dependence of Fibroblast-Like Synoviocytes and Radiation Dose. *J. Immunol. Res.* **2019**, *2019*, 3161750.

(3) Shi, L.; Zhao, Y.; Feng, C.; Miao, F.; Dong, L.; Wang, T.; Stalin, A.; Zhang, J.; Tu, J.; Liu, K.; Sun, W.; Wu, J. Therapeutic effects of shaogan fuzi decoction in rheumatoid arthritis: Network pharmacology and experimental validation. *Front. Pharmacol* **2022**, *13*, 967164.

(4) Han, Z.; Gao, X.; Wang, Y.; Cheng, S.; Zhong, X.; Xu, Y.; Zhou, X.; Zhang, Z.; Liu, Z.; Cheng, L. Ultrasmall iron-quercetin metal natural product nanocomplex with antioxidant and macrophage regulation in rheumatoid arthritis. *Acta Pharm. Sin. B* **2023**, *13* (4), 1726−1739.

(5) Friedman, B.; Cronstein, B. Methotrexate mechanism in treatment of rheumatoid arthritis. *Jt. Bone Spine* **2019**, *86* (3), 301−307.

(6) Zhang, L.; Chen, F.; Geng, S.; Wang, X.; Gu, L.; Lang, Y.; Li, T.; Ye, S. Methotrexate (MTX) Plus Hydroxychloroquine versus MTX Plus Leflunomide in Patients with MTX-Resistant Active Rheumatoid Arthritis: A 2-Year Cohort Study in Real World. *J. Inflammation Res.* **2020**, *13*, 1141−1150.

(7) Singh, J. A. Treatment Guidelines in Rheumatoid Arthritis. *Rheum. Dis. Clin. North Am.* **2022**, *48* (3), 679−689.

(8) Lin, Y. J.; Anzaghe, M.; Schülke, S. Update on the Pathomechanism, Diagnosis, and Treatment Options for Rheumatoid Arthritis. *Cells* **2020**, *9* (4), 880.

(9) Huang, Y.; Gao, X.; An, Y.; Zeng, P.; Chen, C.; Ma, W.; Yao, X. Inhibitory Effect of Jinwujiangu Prescription on Peripheral Blood Osteoclasts in Patients with Rheumatoid Arthritis and the Relevant Molecular Mechanism. *Mediators Inflamm.* **2023**, *2023*, 4814412.

(10) Yi, T.; Zhao, Z. Z.; Yu, Z. L.; Chen, H. B. Comparison of the anti-inflammatory and anti-nociceptive effects of three medicinal plants known as "Snow Lotus" herb in traditional Uighur and Tibetan medicines. *J. Ethnopharmacol.* **2010**, *128* (2), 405.

(11) He, L.; Luan, H.; He, J.; Hu, Y.; Wang, Q. Research progress of Fangji Huangqi Decoction in the treatment of rheumatoid arthritis. *J. Med. Inform.* **2023**, *54* (03), 70−77.

(12) Guan, J.; Wang, L.; Ji, Y.; Zhang, T.; Sang, Y.; Chang, S.; Feng, B.; Zhu, H. UHPLC−MS/MS Method for Quantifying Fangchinoline, Tetrandrine and Calycosin-7-O-β-D-Glucoside of Fangji Huangqi Decoction in Rat Plasma and Its Application to a Pharmacokinetic Study. *J. Chromatogr. Sci.* **2022**, *60* (5), 458−464.

(13) Guo, S.; Yang, L.; Zhang, Q.; Zhang, L.; Li, A. Metabolomics combined with serum pharmacochemistry discovering the potential effective compounds of Fangji Huangqi Tang against nephrotic syndrome. *J. Chromatogr. B Analyt. Technol. Biomed. Life Sci.* **2023**, *1214*, 123532.

(14) Cui, W.; Li, A.; Zhang, L.; Wei, J.; Zhao, Y.; Liu, Y.; Li, K.; Qin, X. Comparison of two different integrated method of pharmacokinetics by the integrated pharmacokinetic research of fangji huangqi decoction. *J. Chromatogr. B Analyt. Technol. Biomed. Life Sci.* **2023**, *1228*, 123831.

(15) Cui, W.; Yang, L.; Zhang, L.; Liu, Y.; Yan, Y.; Li, A.; Qin, X. Rapid Quantitative Analysis of 19 Bioactive Components in Fangji Huangqi Decoction Based on UHPLC-MS/MS. *J. Chromatogr. Sci.* **2023**, *61* (9), 852−862.

(16) Ji, X.; Li, Z.; Hao, H.; Gao, Y. Regulation of Fangji Huangqi Decoction on PI3K-Akt pathway in CIA rat joints. *Chin. J. Immunol.* **2023**, *39* (02), 291−296.

(17) Gao, Y.; Li, Z.; Zhao, Y.; Zhao, C.; Liu, J.; Hao, H. Effect of Fangji Huangqi Decoction on Notch2 /DLL1 Pathway in Joint Tissues of Collageninduced Arthritis Model Rat. *J. Tradit. Chin. Med.* **2021**, *62* (20), 1820−1826.

(18) Fan, J.-Y.; Chen, H.-B.; Zhu, L.; Chen, H.-L.; Zhao, Z.-Z.; Yi, T. Saussurea medusa, source of the medicinal herb snow lotus: a review of its botany, phytochemistry, pharmacology and toxicology. *Phytochem. Rev.* **2015**, *14* (3), 353−366.

(19) Chen, Q.-L.; Chen, X.-Y.; Zhu, L.; Chen, H.-B.; Ho, H.-M.; Yeung, W.-P.; Zhao, Z.-Z.; Yi, T. Review on Saussurea laniceps, a potent medicinal plant known as "snow lotus": botany, phytochemistry and bioactivities. *Phytochem. Rev.* **2016**, *15* (4), 537−565.

(20) Chik, W. I.; Zhu, L.; Fan, L. L.; Yi, T.; Zhu, G. Y.; Gou, X. J.; Tang, Y. N.; Xu, J.; Yeung, W. P.; Zhao, Z. Z.; Yu, Z. L.; Chen, H. B. Saussurea involucrata: A review of the botany, phytochemistry and ethnopharmacology of a rare traditional herbal medicine. *J. Ethnopharmacol.* **2015**, *172*, 44−60.

(21) Yoon, H. Y.; Lee, E. G.; Lee, H.; Cho, I. J.; Choi, Y. J.; Sung, M. S.; Yoo, H. G.; Yoo, W. H. Kaempferol inhibits IL-1β-induced proliferation of rheumatoid arthritis synovial fibroblasts and the production of COX-2, PGE2 and MMPs. *Int. J. Mol. Med.* **2013**, *32* (4), 971−977.

(22) Gao, P.; Rao, Z. W.; Li, M.; Sun, X. Y.; Gao, Q. Y.; Shang, T. Z.; Chen, C.; Zhang, C. L. Tetrandrine Represses Inflammation and Attenuates Osteoarthritis by Selective Inhibition of COX-2. *Curr. Med. Sci.* **2023**, *43* (3), 505−513.

(23) Liu, X. R.; Li, S. F.; Mei, W. Y.; Liu, X. D.; Zhou, R. B. Isorhamnetin Downregulates MMP2 and MMP9 to Inhibit Development of Rheumatoid Arthritis through SRC/ERK/CREB Pathway. *Chin. J. Integr. Med.* **2024**, *30* (4), 299−310.

(24) Fang, J. Y.; Zhu, L.; Yi, T.; Zhang, J. Y.; Yi, L.; Liang, Z. T.; Xia, L.; Feng, J. F.; Xu, J.; Tang, Y. N.; Zhao, Z. Z.; Chen, H. B. Fingerprint analysis of processed Rhizoma Chuanxiong by high-performance liquid chromatography coupled with diode array detection. *Chin. Med.* **2015**, *10*, 2.

(25) Feng, J.; Ren, H.; Gou, Q.; Zhu, L.; Ji, H.; Yi, T. Comparative analysis of the major constituents in three related polygonaceous medicinal plants using pressurized liquid extraction and HPLC-ESI/MS. *Anal. Methods* **2016**, *8* (7), 1557−1564.

(26) Liu, S.; Liang, Q.; Chen, Y.; Li, J.; Shi, Q.; Wang, Y. Simultaneous determination of five constituents in Fangji Huangqi Decoction by HPLC. *Chin. Tradit. Pat. Med.* **2014**, *36* (11), 2312−2315.

(27) Guo, Y.; Fan, Y.; Pei, X. Fangjihuangqi Decoction inhibits MDA-MB-231 cell invasion in vitro and decreases tumor growth and metastasis in triple-negative breast cancer xenografts tumor zebrafish model. *Cancer Med.* **2020**, *9* (7), 2564−2578.

(28) Liu, X.; Zhou, Q.-G.; Zhu, X.-C.; Xie, L.; Cai, B.-C. Screening for Potential Active Components of Fangji Huangqi Tang on the Treatment of Nephrotic Syndrome by Using Integrated Metabolomics Based on "Correlations Between Chemical and Metabolic Profiles. *Front. Pharmacol* **2019**, *10*, 1261.

(29) Li, J.; Zhu, Y.; Zhao, X.; Zhao, L.; Wang, Y.; Yang, Z. Screening of anti-heart failure active compounds from fangjihuangqi decoction in

verapamil-induced zebrafish model by anti-heart failure index approach. *Front. Pharmacol* **2022**, *13*, 999950.
(30) Zhang, C.; Xiang, H.; Wang, J.; Shao, G.; Ding, P.; Gao, Y.; Xu, H.; Ji, G.; Wu, T. Exploring the mechanism of Jianpi Huatan recipe in protecting hepatocellular carcinoma based on network pharmacology. *J. Ethnopharmacol.* **2023**, *317*, 116676.
(31) Zhang, P.; Zhang, D.; Zhou, W.; Wang, L.; Wang, B.; Zhang, T.; Li, S. Network pharmacology: towards the artificial intelligence-based precision traditional Chinese medicine. *Brief. Bioinform.* **2023**, *25* (1), bbad518.
(32) Liu, J.; Tang, J.; Zuo, Y.; Yu, Y.; Luo, P.; Yao, X.; Dong, Y.; Wang, P.; Liu, L.; Zhou, H. Stauntoside B inhibits macrophage activation by inhibiting NF-κB and ERK MAPK signalling. *Pharmacol. Res.* **2016**, *111*, 303−315.
(33) Schett, G.; Zwerina, J.; Firestein, G. The p38 mitogen-activated protein kinase (MAPK) pathway in rheumatoid arthritis. *Ann. Rheum. Dis.* **2008**, *67* (7), 909−916.
(34) Wang, D.; Wu, Z.; Zhao, C.; Yang, X.; Wei, H.; Liu, M.; Zhao, J.; Qian, M.; Li, Z.; Xiao, J. KP-10/Gpr54 attenuates rheumatic arthritis through inactivating NF-κB and MAPK signaling in macrophages. *Pharmacol. Res.* **2021**, *171*, 105496.
(35) Behl, T.; Upadhyay, T.; Singh, S.; Chigurupati, S.; Alsubayiel, A. M.; Mani, V.; Vargas-De-La-Cruz, C.; Uivarosan, D.; Bustea, C.; Sava, C.; Stoicescu, M.; Radu, A. F.; Bungau, S. G. Polyphenols Targeting MAPK Mediated Oxidative Stress and Inflammation in Rheumatoid Arthritis. *Molecules* **2021**, *26* (21), 6570.
(36) Lee, M. R.; Kim, J. E.; Park, J. J.; Choi, J. Y.; Song, B. R.; Choi, Y. W.; Kim, D. S.; Kim, K. M.; Song, H. K.; Hwang, D. Y. Protective role of fermented mulberry leave extract in LPS-induced inflammation and autophagy of RAW264.7 macrophage cells. *Mol. Med. Rep.* **2020**, *22* (6), 4685−4695.
(37) Yuan, W.; Song, H. Y.; Xiong, J.; Jiang, W. L.; Kang, G. J.; Huang, J.; Xie, S. P. Placenta-derived mesenchymal stem cells ameliorate lipopolysaccharide-induced inflammation in RAW264.7 cells and acute lung injury in rats. *Mol. Med. Rep* **2020**, *22* (2), 1458−1466.
(38) Zhu, H.; Wang, X.; Wang, X.; Liu, B.; Yuan, Y.; Zuo, X. Curcumin attenuates inflammation and cell apoptosis through regulating NF-κB and JAK2/STAT3 signaling pathway against acute kidney injury. *Cell Cycle* **2020**, *19* (15), 1941−1951.
(39) Tardito, S.; Martinelli, G.; Soldano, S.; Paolino, S.; Pacini, G.; Patane, M.; Alessandri, E.; Smith, V.; Cutolo, M. Macrophage M1/M2 polarization and rheumatoid arthritis: A systematic review. *Autoimmun. Rev.* **2019**, *18* (11), 102397.
(40) Matsumoto, T.; Takahashi, N.; Kojima, T.; Yoshioka, Y.; Ishikawa, J.; Furukawa, K.; Ono, K.; Sawada, M.; Ishiguro, N.; Yamamoto, A. Soluble Siglec-9 suppresses arthritis in a collagen-induced arthritis mouse model and inhibits M1 activation of RAW264.7 macrophages. *Arthritis Res. Ther.* **2016**, *18* (1), 133.
(41) Lin, W.; Shen, P.; Huang, Y.; Han, L.; Ba, X.; Huang, Y.; Yan, J.; Li, T.; Xu, L.; Qin, K.; Chen, Z.; Tu, S. Wutou decoction attenuates the synovial inflammation of collagen-induced arthritis rats via regulating macrophage M1/M2 type polarization. *J. Ethnopharmacol.* **2023**, *301*, 115802.
(42) da Fonseca, L. J. S.; Nunes-Souza, V.; Goulart, M. O. F.; Rabelo, L. A. Oxidative Stress in Rheumatoid Arthritis: What the Future Might Hold regarding Novel Biomarkers and Add-On Therapies. *Oxid. Med. Cell. Longev.* **2019**, *2019*, 7536805.
(43) Sun, Y.; Liu, J.; Xin, L.; Wen, J.; Zhou, Q.; Chen, X.; Ding, X.; Zhang, X. Xinfeng capsule inhibits inflammation and oxidative stress in rheumatoid arthritis by up-regulating LINC00638 and activating Nrf2/HO-1 pathway. *J. Ethnopharmacol.* **2023**, *301*, 115839.
(44) Liu, J.; Yu, P.; Dai, F.; Jiang, H.; Ma, Z. Tetrandrine reduces oxidative stress, apoptosis, and extracellular matrix degradation and improves intervertebral disc degeneration by inducing autophagy. *Bioengineered* **2022**, *13* (2), 3944−3957.
(45) Kim, S. Y.; Jin, C. Y.; Kim, C. H.; Yoo, Y. H.; Choi, S. H.; Kim, G. Y.; Yoon, H. M.; Park, H. T.; Choi, Y. H. Isorhamnetin alleviates lipopolysaccharide-induced inflammatory responses in BV2 microglia by inactivating NF-κB, blocking the TLR4 pathway and reducing ROS generation. *Int. J. Mol. Med.* **2019**, *43* (2), 682−692.
(46) Tian, M.; Li, N.; Liu, R.; Li, K.; Du, J.; Zou, D.; Ma, Y. The protective effect of licochalcone A against inflammation injury of primary dairy cow claw dermal cells induced by lipopolysaccharide. *Sci. Rep.* **2022**, *12* (1), 1593.

https://doi.org/10.1021/acsomega.4c03495
ACS Omega 2024, 9, 31878−31889